

# On practical robust reinforcement learning: adjacent uncertainty set and double-agent algorithm

Ukjo Hwang, *Student, IEEE*, and Songnam Hong, *Member, IEEE*

**Abstract**—Robust reinforcement learning (RL) aims at learning a policy that optimizes the worst-case performance over an uncertainty set. Given nominal Markov decision process (N-MDP) that generates samples for training, the set contains MDPs obtained by some perturbations from N-MDP. In this paper, we introduce a new uncertainty set containing more realistic MDPs in practice than the existing sets. Using this uncertainty set, we present a robust RL, named ARQ-Learning, for tabular cases. Also, we characterize the finite-time error bounds and prove that it converges as fast as Q-Learning and robust Q-Learning (i.e., the state-of-the-art robust RL method) while providing better robustness for real applications. We propose *pessimistic agent* that efficiently tackles the key bottleneck for the extension of ARQ-Learning into large or continuous state spaces. Using this technique, we first propose PRQ-Learning. To the next, combining this with DQN and DDPG, we develop PR-DQN and PR-DDPG, respectively. We emphasize that our technique can be easily combined with the other popular model-free methods. Via experiments, we demonstrate the superiority of the proposed methods in various RL applications with model uncertainties.

**Index Terms**—Reinforcement learning, robustness, adjacent uncertainty set.

## I. INTRODUCTION

Model-free reinforcement learning (RL) is to learn a policy while interacting with the training environment (simulator model) for decision making problems, in which the environment is modeled as a Markov decision process (MDP) [1], [2]. In RL literature, it is commonly assumed that the training environment is identical to the testing (or true) environment. However, in practice, it is often violated due to the simulator modeling errors (i.e., the mismatch between the simulator and the true environment), environment changes in real system dynamics over time, and unpredictable events. Such model deviation can significantly degrade the real-world performances of the policy learned from the training environment. To address this problem, robust RL has been investigated. The most of existing works can be categorized into the following two approaches. An adversarial training was presented in [3]–[6], where an additional adversarial agent takes an action to hinder the original agent from attaining higher rewards. The behavior of the adversarial agent can mimic the perturbations in the environment. Thus, the original agent can learn a robust policy to some mismatch between the training and testing environments. Another approach is to introduce an uncertainty set containing possible *perturbed* MDPs (or perturbed state transition kernels) from the nominal MDP (N-MDP) (a.k.a. training environment) [7]–[10].

At every time step, a state transition kernel can be changed over the uncertainty set. The objective is to learn a robust

policy that performs well under the *worst-case* MDP in the uncertainty set. Hence, if the uncertainty set is well-designed, an learned policy can guarantee the robustness to some unexpected events in real-world environments.

In this paper, we focus on the second approach to provide the robustness of RL by means of an uncertainty set. Assuming model-free RL, samples (or trajectories) for training are generated from training environment (or nominal MDP (N-MDP)). In many real-world applications, training environment (or simulator) is much easier to collect samples than testing (or true) environment. Whereas, it is inevitable to have some mismatches between training and testing environments. Our goal is twofold: i) design an uncertainty set to capture real-world uncertainties (or perturbations) precisely; ii) learn a robust policy efficiently under the uncertainty set. This is quite demanding since both uncertainty set and an optimal robust policy should be learned simultaneously using samples from N-MDP in an online fashion. Moreover, in robust RL, we need to learn the value functions of the worst-cast MDP in the uncertainty set differently from vanilla RL.

**Related Works.** The framework of robust MDP (i.e., MDP with uncertainty) was first proposed in [11], [12], where a dynamic programming algorithm was proposed to solve the robust MDP. Then, various methods have been presented in [13]–[17]. Nevertheless, the existing studies are restricted by either model-based robust RL or tabular case.

Recently, model-free robust RL has been investigated. In [7], [8], the uncertainty in environment is modeled using confidence region. Using this uncertainty set, the authors developed robust RL algorithm based on linear function approximation. In model-free RL (i.e., N-MDP is unknown), however, it is hard to find a confidence region which is determined by some constraints on probability distributions. Consequently, they failed to find an optimal robust policy efficiently under this uncertainty set. Instead, they introduced a proxy confidence region which is obtained by relaxing some conditions in the confidence region. Based on this, they developed an efficient robust RL method. However, there is no theoretical guarantee for the exactness of this approximation.

In [9], [10], robust RL method was developed using *R*-contamination [18]–[24] uncertainty set, which is the most related work of this paper. Differently from [7], [8], this uncertainty set does not require any condition for probability distributions. This makes it possible to construct model-free robust RL method without any relaxation. However, this uncertainty set still poses the problem of including several unrealistic perturbed MDPs (i.e., unrealistic state transition probabilities). In real-world applications, these unrealistic ones

are indeed infeasible (see Section III-A for details). Moreover, their experiments were very limited and did not extend to continuous action space environments.. These limitations are the motivation of our work.

**Contributions.** We first present an *adjacent R-contamination* set as an elaboration of the uncertainty set in [9], [10] in a more practical way. As aforementioned, the existing uncertainty set contains some unrealistic perturbations as it allows any current state to transmit to every state in the state space. Whereas, our uncertainty set only allows to transit to neighboring states having non-zero transition probabilities in N-MDP (or training environment).

Based on the proposed uncertainty set, we develop the sample-based method, named ARQ-Learning for tabular case. We conduct the analytical analysis for ARQ-Learning and show that it converges as fast as the vanilla Q-Learning [25] and robust Q-Learning [9] while ensuring the robustness to more practical uncertainty in environment.

Applying ARQ-Learning to robust RL with large state and action spaces is intractable as it requires large memory space. The major challenge to solve an maximization problem induced by the proposed uncertainty set. We tackle this problem by presenting a novel robust Q-Learning, named PRQ-Learning. The main idea is to introduce an additional *pessimistic agent* whose objective is to efficiently solve the aforementioned maximization problem in an online and incremental fashion. Incorporating the idea of pessimistic agent to other model-free RL methods as DQN [26] and DDPG [27], we develop PR-DQN for continuous state space and PR-DDPG for continuous state and action spaces, which enables robust RL to be adopted in various real-world applications.

Via experiments, we demonstrate the superiority of the proposed methods compared with the previous methods. It is shown that our algorithms indeed ensure the robustness against action or parameter perturbations in environment. Additionally, the proposed methods achieve much higher rewards than vanilla RL method and robust RL methods.

## II. PRELIMINARIES

In this section, we provide some definitions that will be used throughout the paper and formally define a robust reinforcement learning (RL) with model uncertainty.

**MDP.** A Markov decision process (MDP) is defined with a tuple  $(\mathcal{S}, \mathcal{A}, \mathbf{P} = (p_{s,s'}^a), c, \gamma)$ , where  $\mathcal{S}$  is the state space,  $\mathcal{A}$  is the action space,  $\mathbf{P}$  is the state transition kernel,  $c : \mathcal{S} \times \mathcal{A} \rightarrow \mathbb{R}$  is the cost function, and  $\gamma \in (0, 1)$  is the discount factor. Here,  $p_{s,s'}^a$  represents the probability of transition to state  $s' \in \mathcal{S}$  when action  $a \in \mathcal{A}$  is taken at the current state  $s \in \mathcal{S}$ . For ease of notation, we let  $p_s^a = (p_{s,s'}^a)$  denote the probability distribution on the possible next state  $s' \in \mathcal{S}$ , given the current state  $s$  and action  $a$ . At every time step  $t$ , an agent observes the environment's state  $s_t$  and takes an action  $a_t$  according to the agent's policy  $\pi : \mathcal{S} \times \mathcal{A} \rightarrow [0, 1]$ . Then, the environment moves to a next state  $s_{t+1}$  according to  $p_{s_t, s_{t+1}}^{a_t}$  and generates

a cost  $c(s_t, a_t)$ . Given a state  $s \in \mathcal{S}$ , the value function of a policy  $\pi$  is evaluated as

$$V_{\pi, \mathbf{P}}^{\pi}(s) = \mathbb{E}_{\pi, \mathbf{P}} \left[ \sum_{t=0}^{\infty} \gamma^t c(s_t, a_t) \middle| s_0 = s \right], \quad (1)$$

where  $a_t \sim \pi(s_t)$  and  $s_{t+1} \sim p_{s_t}^{a_t}$ . Given the MDP  $(\mathcal{S}, \mathcal{A}, \mathbf{P} = (p_{s,s'}^a), c, \gamma)$ , the objective of RL is to find an optimal policy  $\pi^*$  such that  $\pi^* = \operatorname{argmin}_{\pi} V_{\pi, \mathbf{P}}^{\pi}(s), \forall s \in \mathcal{S}$ .

**Robust MDP.** In robust MDP, there is some uncertainty in an environment for which the state transition kernel  $\mathbf{P}$  is not fixed but can be changed (or perturbed) at every time step. This uncertainty can be captured by an uncertainty set  $\mathcal{P}$  that contains all possible *perturbed* state transition kernels. As in [11], [12], it is commonly assumed that the uncertainty set has the form of  $\mathcal{P} = \bigotimes_{(s,a) \in \mathcal{S} \times \mathcal{A}} \mathcal{P}_{s,a}^a$ ,

where  $\mathcal{P}_{s,a}^a$  includes all perturbed transition distributions of a next state  $s'$  given the current state  $s$  and action  $a$ . Given the set  $\mathcal{P}$ , a robust MDP (**R-MDP**) is specified as  $(\mathcal{S}, \mathcal{A}, \mathcal{P}, c, \gamma)$ . As aforementioned, in robust RL, the training environment (a.k.a., nominal MDP (**N-MDP**))  $(\mathcal{S}, \mathcal{A}, \bar{\mathbf{P}} = (\bar{p}_{s,s'}^a), c, \gamma)$  is defined, from which samples for training are assumed to be generated. Let  $\mathbf{P}_t$  be the state transition kernel at time step  $t$  and  $\kappa = (\mathbf{P}_0, \mathbf{P}_1, \dots)$  be a sequence of time-varying state transition kernels.

In robust RL, one key challenge is to build an uncertainty set such that i) it can reflect real-world mismatches; ii) it is manageable to find an optimal robust policy via an efficient algorithm. We contribute to this subject in Section III - Section V. Given an uncertainty set  $\mathcal{P}$ , robust RL seeks an optimal robust policy  $\pi^*$  to minimize the cumulative discounted cost over all state transition kernels in the uncertainty set. In the remaining part of this section, we provide some definitions and notations that will be used to tackle the above problem. Given the state  $s$ , the *robust* state value function of a policy  $\pi$  is defined as

$$V^{\pi}(s) = \max_{\kappa} \mathbb{E}_{\pi, \kappa} \left[ \sum_{t=0}^{\infty} \gamma^t c(s_t, a_t) \middle| s_0 = s \right], \quad (2)$$

where  $\mathbb{E}_{\kappa}$  denotes the expectation when state transitions follow  $\kappa$ . Also, given the state  $s$  and action  $a$ , the *robust* action value function of a policy  $\pi$  is defined as

$$Q^{\pi}(s, a) = \max_{\kappa} \mathbb{E}_{\pi, \kappa} \left[ \sum_{t=0}^{\infty} \gamma^t c(s_t, a_t) \middle| s_0 = s, a_0 = a \right]. \quad (3)$$

The optimal policy of robust MDP is defined as  $\pi^* = \operatorname{argmin}_{\pi} V^{\pi}(s), \forall s \in \mathcal{S}$ .

For the ease of expositions, we let  $V^*$  and  $Q^*$  denote the optimal value functions, which implies  $V^{\pi^*}$  and  $Q^{\pi^*}$ , respectively. The optimal value functions have the relation such as  $V^* = \min_{a \in \mathcal{A}} Q^*(s, a)$ .

## III. THE PROPOSED ROBUST RL

In this section, we introduce a new uncertainty set which is more practical and precise than the existing sets. Then, we derive the robust Bellman operator  $\mathbf{T}$  for the proposed uncertainty set  $\mathcal{P}$ .

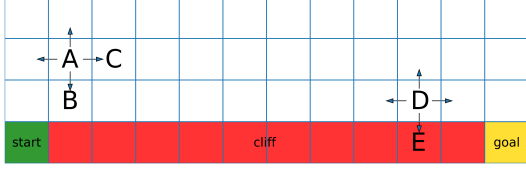


Fig. 1. A grid-world with cliff (or CliffWalking-v0), where agent's aim is to reach the goal. Here, green represents start state, yellow represents goal, and red represents cliff which gives highest cost.

#### A. The Proposed Uncertainty Set

In this section, we describe the proposed uncertainty set for robust RL. Since model-free robust RL is considered (i.e., N-MDP is unknown), it is unable to generate samples (or trajectories) directly from a time-varying model  $\mathbf{P}_t \in \mathcal{P}$ . In the design of an uncertainty set, thus, it should be considered to develop an efficient way to mimic such samples only using the samples from N-MDP. Namely, it is demanding to train a robust agent from R-MDP with a general uncertainty set. For this reason, the two kinds of tractable uncertainty sets have been widely used. First, the uncertainty set based on a confidence region was presented in [7], [8]: for  $\forall(s, a) \in \mathcal{S} \times \mathcal{A}$ ,

$$\mathcal{P}_s^a \triangleq \{\bar{p}_s^a + u \mid u \in \mathcal{U}_s^a\}, \quad (4)$$

where  $\mathcal{U}_s^a = \{x \mid \|x\|_2 \leq R, \sum_{s' \in \mathcal{S}} x_{s'} = 0, -\bar{p}_{s,s'}^a \leq x_{s'} \leq 1 - \bar{p}_{s,s'}^a, \forall s' \in \mathcal{S}\}$ . Next, the so-called  $R$ -contamination uncertainty set was introduced in [9], [10]: for  $\forall(s, a) \in \mathcal{S} \times \mathcal{A}$ ,

$$\mathcal{P}_s^a \triangleq \{(1 - R)\bar{p}_s^a + Rq \mid q \in \Delta_{|\mathcal{S}|}\}, \quad (5)$$

where  $\Delta_{|\mathcal{S}|}$  is the  $(|\mathcal{S}| - 1)$ -dimensional probability simplex. In the both sets, the state transition probability  $\bar{p}_s^a$  from N-MDP is used as the centroid and  $R \in [0, 1]$  denotes a robustness level. For these uncertainty sets, model-free robust RL has been well-investigated [7]–[10].

Nevertheless, these uncertainty sets have the limitation to describe real-world environments. Generally, in real environments, a state  $s$  cannot transit to every state  $s' \in \mathcal{S}$ . In the example of CliffWalking (see Figure 1), an agent can only move in 4 directions, i.e., it can only reach to 4 neighboring states. When the uncertainty set in (4) or (5) is used, however, the most of MDPs in the uncertainty set enables that any state  $s$  can transit to the entire states with non-zero probabilities. Such unrealistic transitions can occur since the existing uncertainty sets are improperly designed, i.e., the constraints for  $u$  in (4) and  $q$  in (5) are inadequate.

This motivates us to present a new uncertainty set, named *adjacent  $R$ -contamination uncertainty set*:

**Definition 1.** Given N-MDP  $(\mathcal{S}, \mathcal{A}, \bar{\mathbf{P}} = (\bar{p}_{s,s'}^a), c, \gamma)$  which generates samples for training, we define an *adjacent  $R$ -contamination uncertainty set*: for  $\forall(s, a) \in \mathcal{S} \times \mathcal{A}$ ,

$$\mathcal{P}_s^a \triangleq \{(1 - R)\bar{p}_s^a + Rq \mid q \in \mathcal{Q}_s\}, \quad (6)$$

where  $\mathcal{Q}_s \triangleq \{q \in \Delta_{|\mathcal{S}|} \mid q_{s'} = 0, \forall s' \in \mathcal{S} - \mathcal{N}_s\} \subseteq \Delta_{|\mathcal{S}|}$  contains all feasible conditional distributions

and the neighboring set of a state  $s \in \mathcal{S}$  is defined as  $\mathcal{N}_s \triangleq \{s' \in \mathcal{S} \mid \sum_{a \in \mathcal{A}} \bar{p}_{s,s'}^a \neq 0\}$ .

Note that when  $R = 0$ ,  $\mathcal{P}$  is the singleton with  $\{\bar{\mathbf{P}}\}$ , i.e., in this case, robust RL is reduced to vanilla RL.

Clearly, the proposed uncertainty set is the subset of the  $R$ -contamination uncertainty set in (5). We argue that the former only includes realistic state transition probabilities from the latter, given the premise that infeasible transitions in N-MDP are more likely to be still infeasible in perturbed environments. For example, in Figure 1, suppose that an agent at the state 'A' tries to move to the state 'C'. Due to the environment's uncertainty (e.g., action perturbations), the agent can move to unwanted state 'B'. However, it is unreasonable to assume that the agent at the state 'A' can move to the state 'D' or 'E' directly in one step. This unrealistic movement is prevented in our uncertainty set, whereas it is allowed with non-zero probability in the existing uncertainty sets in (4) and (5). Therefore, the proposed uncertainty set in (6) can reflect real-world environments more elaborately than the existing ones. Also, in Section IV and Section V, the implementation feasibility of the proposed uncertainty set will be verified by manifesting that it will be well-integrated with the state-of-the-art RL methods.

#### B. Robust Bellman Operator

Bellman operator is commonly used in RL algorithm for policy evaluation steps. Similarly, we need to define a robust Bellman operator for the robust MDP. In [28], given an uncertainty set  $\mathcal{P}_s^a$ , the robust Bellman operator is defined as  $\mathbf{T}Q^\pi(s, a) = c(s, a) + \gamma \sigma_{\mathcal{P}_s^a}(V^\pi)$ ,

where  $\sigma_{\mathcal{P}_s^a}(v) \triangleq \max_{p \in \mathcal{P}_s^a} p^\top v$  denotes support function of  $\mathcal{P}_s^a$ . Note that this Bellman operator holds for the uncertainty sets in (4), (5), and (6). Particularly, the robust Bellman operator for our uncertainty set in (6) is defined as

$$\begin{aligned} \mathbf{T}Q^\pi(s, a) = & c(s, a) + \gamma(1 - R) \left[ \sum_{s' \in \mathcal{S}} \bar{p}_{s,s'}^a V^\pi(s') \right] \\ & + \gamma R \left[ \max_{s' \in \mathcal{N}_s} V^\pi(s') \right], \end{aligned} \quad (7)$$

where  $R \in [0, 1]$  is a robustness-level,  $\mathcal{Q}_s$  and  $\mathcal{N}_s$  are given in Definition 1.

We analyze the convergence of our robust Bellman operator in (7) below:

**Theorem 1.** For any  $\gamma \in (0, 1)$  and  $R \in [0, 1]$ , the Bellman operator  $\mathbf{T}$  in (7) is a contraction with respect to  $l_\infty$ -norm, and the robust value function  $Q^\pi$  is its unique fixed point.

**Proof.** The proof is provided in Appendix A.

From (7), we will design sample-based robust RL methods for tabular and function-approximation cases in Section IV and Section V, respectively.

## IV. PROPOSED TABULAR METHODS

In this section, we focus on the tabular case with finite state and action spaces.

### A. ARQ-Learning

Leveraging the robust Bellman operator in (7), it can be expected to develop Q-Learning method. However, unlike vanilla RL, the maximization over neighboring states in (7) should be efficiently tackled. For this, during training, two requirements should be addressed: i) given a state  $s \in \mathcal{S}$ , the neighboring set  $\mathcal{N}_s$  should be identified using the samples from the training environment; ii) using the neighboring set  $\mathcal{N}_s$ , the maximization in (7) should be efficiently solved.

First, to identify neighboring sets  $\mathcal{N}_s$  for  $\forall s \in \mathcal{S}$ , we define an indicator transition matrix (ITM), denoted by  $\mathbf{B} \in \{0, 1\}^{|\mathcal{S}| \times |\mathcal{S}|}$ , where the  $(i, j)$ -component of  $\mathbf{B}$  (i.e.  $\mathbf{B}_{i,j}$ ) is equal to 1 if the state transition from the state  $i$  to the state  $j$  can occur with non-zero probability. During training, this matrix is estimated using samples. For instance, starting with all-zero matrix,  $\mathbf{B}_{i,j}$  is set by 1 as long as the sample that transit the state  $i$  to the state  $j$  occurs. From the ITM  $\mathbf{B}$ , we can build an estimated neighboring set as  $\hat{\mathcal{N}}_s = \{s' \in \mathcal{S} \mid \mathbf{B}_{s,s'} \neq 0\}$ . Clearly, we have that  $\hat{\mathcal{N}}_s \subseteq \mathcal{N}_s$  and after enough time steps,  $\hat{\mathcal{N}}_s \approx \mathcal{N}_s$  for  $\forall s \in \mathcal{S}$ . From the estimated neighboring sets and the robust Bellman operator in (7), we can develop the update of our robust Q-Learning with sample  $(s_t, a_t, c_t = c(s_t, a_t), s_{t+1})$ :

$$Q_{t+1}^\pi(s_t, a_t) \leftarrow (1 - \alpha)Q_t^\pi(s_t, a_t) + \alpha \left( c_t + \gamma R \max_{s' \in \hat{\mathcal{N}}_{s_t}} V_t^\pi(s') + \gamma(1 - R)V_t^\pi(s_{t+1}) \right), \quad (8)$$

where  $\alpha > 0$  is a learning rate. Leveraging the update in (8), we propose Adjacent Robust Q-Learning (ARQ-Learning) in Algorithm 1. Remarkably, it can perform only using samples from training environment. When  $R = 0$ , this method is reduced to vanilla Q-Learning. To compare with the most related work [9], the update of robust Q-Learning (using  $R$ -contamination uncertainty set) is defined as follows:

$$Q_{t+1}^\pi(s_t, a_t) \leftarrow (1 - \alpha)Q_t^\pi(s_t, a_t) + \alpha \left( c_t + \gamma R \max_{s' \in \mathcal{S}} V_t^\pi(s') + \gamma(1 - R)V_t^\pi(s_{t+1}) \right). \quad (9)$$

In comparison with the update of ARQ-Learning in (8), we observe that there is no constraint for the maximization in (9). This difference makes robust Q-Learning unable to consider an uncertainty in environment properly. Consider the example of Figure 1, where the state ‘E’ is likely to have higher value  $V_t^\pi(s = \text{‘E’})$  as it is in the cliff. When evaluating the action value function at the state ‘D’, it makes sense to consider  $V_t^\pi(\text{‘E’})$  as the state ‘D’ has some possibility to move to the neighboring state ‘E’ by some unexpected events. However, when evaluating the action value function at the state ‘A’, it is unreasonable to take  $V_t^\pi(\text{‘E’})$  into account since the state ‘A’ is far from the state ‘E’. Nevertheless, it is considered when evaluating (9) at the state ‘A’ in robust Q-Learning [9]. This problem has been perfectly addressed in the update of ARQ-Learning in 8. Namely, ARQ-Learning only considers the realistic danger caused by neighboring states when evaluating the action value function in (8). Moreover, suppose that  $V_t^\pi(\text{‘E’})$  is extremely high, which is highly likely to occur. Then, the maximum state ‘E’ =  $\arg\max_{s \in \mathcal{S}} V_t^\pi(s)$  in

(9) could be the same for the entire time steps. At every state, the almost same value is added, which is nothing but adding a constant at every time steps. Due to the aforementioned reasons, it can be understood that the proposed set better takes into account an uncertainty in environment.

We conduct a theoretical analysis to derive the finite-time error bound of the proposed ARQ-Learning. Before stating our main result, we provide some useful notations and assumption. Let  $\mu_{\pi_b}$  be the stationary distribution over  $\mathcal{S} \times \mathcal{A}$  induced by behavior policy  $\pi_b$ . Given  $\mu_{\pi_b}$ ,

we define the  $\mu_{\min} = \min_{(s,a) \in \mathcal{S} \times \mathcal{A}} \mu_{\pi_b}(s, a)$  and  $t_{\text{mix}} = \min\{t : \max_{s \in \mathcal{S}, a \in \mathcal{A}} d_{\text{TV}}(\mu_{\pi_b}, p_s^a) \leq 0.25\}$ , where  $d_{\text{TV}}$  is the total variation distance.

**Assumption 1.** The Markov chain induced by the stationary behavior policy  $\pi_b$  and the state transition kernel  $\bar{p}_s^a, \forall (s, a) \in \mathcal{S} \times \mathcal{A}$  is uniformly ergodic.

This assumption is commonly used in the analysis of vanilla Q-Learning [25] and the existing robust Q-Learning in [9].

**Theorem 2.** Under Assumption 1, there exist some constants  $c_0, c_1 > 0$ , such that for any  $0 < \delta < 1$  and  $0 < \varepsilon \leq \frac{1}{1-\gamma}$ , ARQ-Learning with the learning rate  $\alpha = \frac{c_1}{\log\left(\frac{|\mathcal{S}||\mathcal{A}|T}{\delta}\right)} \min\left(\frac{1}{t_{\text{mix}}}, \frac{(1-\gamma)^4 \varepsilon^2}{\gamma^2}\right)$  satisfies the following bound with probability at least  $1 - \delta$ :

$$|Q_T(s, a) - Q^*(s, a)| \leq \varepsilon, \quad \forall (s, a) \in \mathcal{S} \times \mathcal{A}, \quad (10)$$

provided that  $T$  satisfies

$$T \geq \frac{c_0}{\mu_{\min}} \left( \frac{1}{(1-\gamma)^5 \varepsilon^2} + \frac{t_{\text{mix}}}{(1-\gamma)} \right) \times \log \left( \frac{|\mathcal{S}||\mathcal{A}|T}{\delta} \right) \log \left( \frac{1}{(1-\gamma)^2 \varepsilon} \right).$$

**Proof.** The proof is provided in Appendix B.

From Theorem 2, we can identify that a sample size  $\tilde{\mathcal{O}}\left(\frac{1}{\mu_{\min}(1-\gamma)^5 \varepsilon^2} + \frac{t_{\text{mix}}}{\mu_{\min}(1-\gamma)}\right)$  is required to guarantee an  $\varepsilon$ -accuracy. The complexity of ARQ-Learning is well-matched with vanilla Q-learning in [25] and robust Q-Learning in [9] while ensuring the robustness to practical model uncertainties. Despite its effectiveness, ARQ-Learning can suffer from the large memory space to store the ITM  $\mathbf{B}$  especially when state space becomes large. This problem will be addressed in the subsequent subsection by introducing pessimistic agent.

### B. PRQ-Learning

As explained in Section IV-A, ARQ-Learning is not practical when state space is large. We address this problem by solving the maximization in (7) without explicitly identifying neighboring sets (i.e., without constructing the ITM  $\mathbf{B}$ ). Toward this, we introduce an additional agent (named pessimistic agent) whose learned policy can directly give the solution of the maximization in (7). Moreover, pessimistic agent can be trained only using the samples from N-MDP (i.e., the training environment). Thus, both original (or robust) and pessimistic agents can be trained simultaneously although they have totally different objectives.

**Pessimistic Agent.** This agent aims at solving the maximization in (7). From the cost function of robust agent

**Algorithm 1** ARQ-Learning

---

```

1: Input: Learning rate  $\alpha > 0$ , discounted factor  $\gamma \in (0, 1)$ ,
   and robustness-level  $R$ .
2: Initialization:  $Q^\pi(\cdot, \cdot)$ ,  $\mathbf{B} = \mathbf{0}$ ,  $s_0 \in \mathcal{S}$ .
3: for each epoch do
4:   for each environment step do
5:      $a_t \sim \pi(s_t)$  and  $s_{t+1} \sim \bar{p}_{s_t}^{a_t}$ 
6:      $\mathcal{D} \leftarrow \mathcal{D} \cup \{(s_t, a_t, c_t, s_{t+1})\}$ 
7:      $\mathbf{B}_{s_t, s_{t+1}} \leftarrow 1$  and  $s_t \leftarrow s_{t+1}$ 
8:   end for
9:   for each update step do
10:     $(s, a, c, s') \sim \mathcal{D}$ 
11:     $V_t^\pi(s') = \min_{a' \in \mathcal{A}} Q_t^\pi(s', a')$ 
12:    Update  $Q^\pi$  via (8)
13:   end for
14: end for

```

---

$c(s, a)$ , the reward function of pessimistic agent is define as  $c^p(s, a) = -c(s, a)$ . Also, let  $\phi$  be the policy of pessimistic agent. Then, the value functions for pessimistic agent are defined as

$$V^\phi(s) = \mathbb{E}_{\phi, \mathbf{P}} \left[ \sum_{t=0}^{\infty} \gamma^t c^p(s_t, a_t) \middle| s_0 = s \right]$$

$$Q^\phi(s, a) = \mathbb{E}_{\phi, \mathbf{P}} \left[ \sum_{t=0}^{\infty} \gamma^t c^p(s_t, a_t) \middle| s_0 = s, a_0 = a \right].$$

Then, the optimal policy of pessimistic agent is obtained as  $\phi^* = \operatorname{argmin}_{\phi} V^\phi(s)$ ,  $\forall s \in \mathcal{S}$ .

To distinguish from the state and action of robust agent, we let  $x_t \in \mathcal{S}$  and  $u_t \in \mathcal{A}$  be the state and action of pessimistic agent at time step  $t$ . Then, using the sample  $(x_t, u_t, c_t^p = c^p(x_t, u_t), x_{t+1})$ , the Q-Learning update for pessimistic agent is obtained as

$$Q_{t+1}^\phi(x_t, u_t) \leftarrow (1 - \alpha) Q_t^\phi(x_t, u_t) + \alpha \left( c_t^p + V_t^\phi(x_{t+1}) \right), \quad (11)$$

where  $\alpha > 0$  is a learning rate. Note that this update is equivalent to that of the vanilla Q-Learning except for cost function. However, in the training of pessimistic agent, the following should be carefully taken into account.

Pessimistic agent aims at maximizing the cumulative cost as the opposite of robust agent. As manifested in RL, the maximum cost tends to terminate an episode early, thereby hindering pessimistic agent from exploring states sufficiently. This makes the training of pessimistic agent intractable. We address this problem by means of the *state-sharing* technique, wherein the current state of pessimistic agent is coupled with that of robust agent. To harness the exploration ability of robust agent, pessimistic agent is trained in the following ways: at every time step, before interacting with the training environment, the current state of the pessimistic agent is updated as that of robust agent (i.e.,  $x_t = s_t$ ). Due to the state-sharing, in (11), the current state  $x_t$  can be replaced with  $s_t$ . The details of this training are described in Algorithm 2.

Remarkably, the devise of pessimistic agent enables to extend robust RL with the proposed uncertainty set into continuous state and action spaces.

**Robust Agent.** At every time step  $t$ , the tuple  $(s_t, a_t, c_t, s_{t+1}, u_t, c_t^p, x_{t+1})$  is sampled, where  $x_t = s_t$  via the state-sharing. By construction, the action of pessimistic agent  $u_t$  is sampled so that the corresponding next state  $x_{t+1}$  is likely to solve the maximization in (7) directly, i.e.,  $\max_{s' \in \mathcal{N}_{s_t}} V^\pi(s') \approx V^\pi(x_{t+1})$ . This is verified via experiments (see Figure. 1 in Appendix D). Now we have solved the challenging part of the robust Bellman operator in (7) just using samples from the training environment. Then, the Q-Learning update for the robust agent is given as

$$Q_{t+1}^\pi(s_t, a_t) \leftarrow (1 - \alpha) Q_t^\pi(s_t, a_t) + \alpha (c_t + \gamma R \cdot V_t^\pi(x_{t+1}) + \gamma(1 - R) V_t^\pi(s_{t+1})), \quad (12)$$

where  $x_{t+1}$  is provided by pessimistic agent. Leveraging the updates in (11) and (12), we present Pessimistic Robust Q-Learning (PRQ-Learning) in Algorithm 2. One might concern that when training is premature, pessimistic agent cannot find an exact solution of the maximization in (7), i.e.,  $V^\pi(x_{t+1}) < \max_{s' \in \mathcal{N}_{s_t}} V^\pi(s')$ . However, it is at least guaranteed that pessimistic agent gives the state value of a certain neighboring state, i.e.,  $V^\pi(x_{t+1}) = V^\pi(s)$  for some  $s \in \mathcal{N}_{s_t}$ , thereby yielding more precise value than  $\max_{s' \in \mathcal{S}} V_t^\pi(s')$  in (9). As training proceeds, furthermore, pessimistic agent tends to find an action that can lead to solution of  $\max_{s' \in \mathcal{N}_{s_t}} V^\pi(s')$ . Noticeably, the proposed PRQ-Learning can perform only using the samples from the training environment, whereas the existing methods in [7]–[10] requires some additional hard computations.

**Algorithm 2** PRQ-Learning

---

```

1: Input: Learning rate  $\alpha > 0$ , discounted factor  $\gamma \in (0, 1)$ ,
   and robustness-level  $R$ .
2: Initialization:  $Q^\pi(\cdot, \cdot)$ ,  $Q^\phi(\cdot, \cdot)$ ,  $s_0 \in \mathcal{S}$ .
3: for each epoch do
4:   for each environment step do
5:      $x_t \leftarrow s_t$ ,  $a_t \sim \pi(s_t)$ , and  $u_t \sim \phi(x_t)$ 
6:      $s_{t+1} \sim \bar{p}_{s_t}^{a_t}$  and  $x_{t+1} \sim \bar{p}_{x_t}^{u_t}$ 
7:      $c_t = c(s_t, a_t)$  and  $c_t^p = -c(x_t, u_t)$ 
8:      $\mathcal{D} \leftarrow \mathcal{D} \cup \{(s_t, a_t, c_t, s_{t+1}, u_t, c_t^p, x_{t+1})\}$ 
9:      $s_t \leftarrow s_{t+1}$ 
10:   end for
11:   for each update step do
12:     $(s, a, c, s', u, c^p, x') \sim \mathcal{D}$ 
13:     $V_t^\pi(x') = \min_{a' \in \mathcal{A}} Q_t^\pi(x', a')$ 
14:     $V_t^\pi(s') = \min_{a' \in \mathcal{A}} Q_t^\pi(s', a')$ 
15:     $V_t^\phi(x') = \min_{u' \in \mathcal{A}} Q_t^\phi(x', u')$ 
16:    Update  $Q^\phi$  via (11) and  $Q^\pi$  via (12)
17:   end for
18: end for

```

---

## V. PROPOSED FUNCTION APPROXIMATION METHODS

In this section, we extend the proposed PRQ-Learning into more practical cases that state and action spaces are

large or even continuous. This extension is made by appropriately incorporating the idea of pessimistic agent into the popular function-approximation methods such as deep-Q network (DQN) [26] and deep deterministic policy gradient (DDPG) [27]. The resulting methods are respectively named Pessimistic Robust DQN (PR-DQN) and Pessimistic Robust DDPG (PR-DDPG). The detailed procedures of PR-DQN and PR-DDPG are respectively provided in Algorithm 1 and 2 in Appendix C. Following the notations in PRQ-Learning, let  $s$  and  $a$  denote the state and action of robust agent, respectively. Also, let  $x$  and  $u$  denote the state and action of pessimistic agent, respectively. Using the state-sharing, the tuple  $(s = x, a, c, s', u, c^p, x')$  is sampled from the replay buffer.

**PR-DQN.** We propose PR-DQN for robust RL by incorporating the idea of pessimistic agent in Section IV-B into DQN. In the proposed method, we define the two Q-networks, named robust Q-network and pessimistic Q-network for robust and pessimistic agents, respectively. The loss function of the pessimistic Q-network (denoted by  $Q^\phi(x, u; \psi)$ ) is defined as follows:

$$L_{Q^\phi}(\psi) = \mathbb{E}_{(x, u, c^p, x') \sim \mathcal{D}} [(Q^\phi(x, u; \psi) - y)^2], \quad (13)$$

where  $y = c^p + \gamma \bar{V}^\phi(x')$ , and  $\bar{V}^\phi$  is target network.

Also, the loss function of robust Q-network (denoted by  $Q^\pi(s, a; \omega)$ ) is defined as follows:

$$L_{Q^\pi}(\omega) = \mathbb{E}_{(s, a, c, s', x') \sim \mathcal{D}} [(Q^\pi(s, a; \omega) - y)^2], \quad (14)$$

where  $y = c + \gamma(R\bar{V}^\pi(x') + (1 - R)\bar{V}^\pi(s'))$  and  $\bar{V}^\pi$  is target network. Note that like PRQ-Learning, the Q-networks are trained only using the samples from the training environment.

**PR-DDPG.** We propose PR-DDPG for robust RL by incorporating the idea of pessimistic agent in Section IV-B into DDPG. In the proposed method, we define the four DNNs such as  $Q^\pi(s, a; \omega)$  and  $\pi(s; \theta)$  for robust agent and  $Q^\phi(x, u; \psi)$  and  $\phi(x; \sigma)$  for pessimistic agent. Namely, during training, the parameters  $\omega$ ,  $\theta$ ,  $\psi$ , and  $\sigma$  should be estimated simultaneously. Since, in PR-DDPG, the loss functions for Q-networks are exactly same as PR-DQN, we can use the loss functions in (13) for  $Q^\phi$  and (14) for  $Q^\pi$ , respectively. Thus, we only need to provide the loss functions for policy networks. The loss function of policy-network for pessimistic agent (denoted by  $\phi(x; \sigma)$ ) is defined as

$$L_\phi(\sigma) = \mathbb{E}_{x \sim \mathcal{D}} [Q^\phi(x, u; \psi) |_{u=\phi(x; \sigma)}]. \quad (15)$$

Also, the loss function of policy-network for robust agent (denoted by  $\pi(s; \theta)$ ) is defined as

$$L_\pi(\theta) = \mathbb{E}_{s \sim \mathcal{D}} [Q^\pi(s, a; \omega) |_{a=\pi(s; \theta)}]. \quad (16)$$

Note that both loss functions are the same as vanilla DDPG [27]. However, since Q-networks are trained according to the robust Bellman operator in (7), robust agent in PR-DDPG is able to learn a robust action compared with the vanilla counterpart.

While we used DQN and DDPG as the baseline RL methods, one can easily incorporate the idea of pessimistic agent

into the other model-free RL methods (e.g., SAC [29] and PPO [30]). Specifically, the value function of robust agent is trained using the modified loss function according to the robust Bellman operator in (7). Also, pessimistic agent can be trained in the same way as PR-DQN in discrete action space or PR-DDPG in continuous action space.

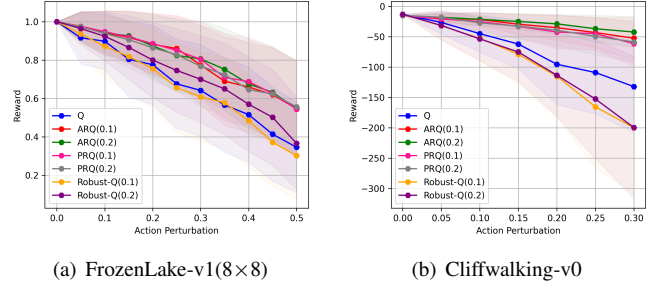


Fig. 2. Performance comparisons of various tabular methods under action perturbations. Here, FrozenLake-v1 is set as non-slippery.

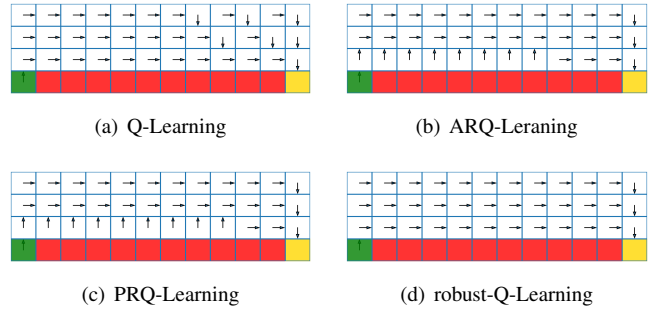


Fig. 3. Optimal actions in CliffWalking-v0, where green, red, and yellow colors denote start, cliff, and goal states, respectively.

## VI. EXPERIMENT

We conduct the experiments to validate the superiority of the proposed methods. As benchmark methods, we consider the vanilla RL methods such as Q-Learning, DQN, and DDPG since they are used as the baseline methods of ours. Also, to compare with the state-of-the-art robust RL methods, we implement robust Q-Learning (in short, Robust-Q) [9] for tabular case. Regarding continuous state spaces, we implement Robust-DQN and Robust-DDPG (in short, R-DQN and R-DDPG) by combining DQN and DDPG with the  $R$ -contamination uncertainty set in [9], [10]. As aforementioned, it is hard to find the maximum in (9) precisely. Thus, we estimate it by taking the maximum among stored values in the value memory. OpenAI gym [31] is used for various environments.

In our experiments, an agent is trained from training environment. Then, our learned agent is evaluated from testing environment (i.e., training environment with some perturbations). Among various types of perturbations, we consider action and parameter perturbations. First, action perturbation implies that an agent can take a random action with some probability instead of an optimal action (provided by a learned policy).



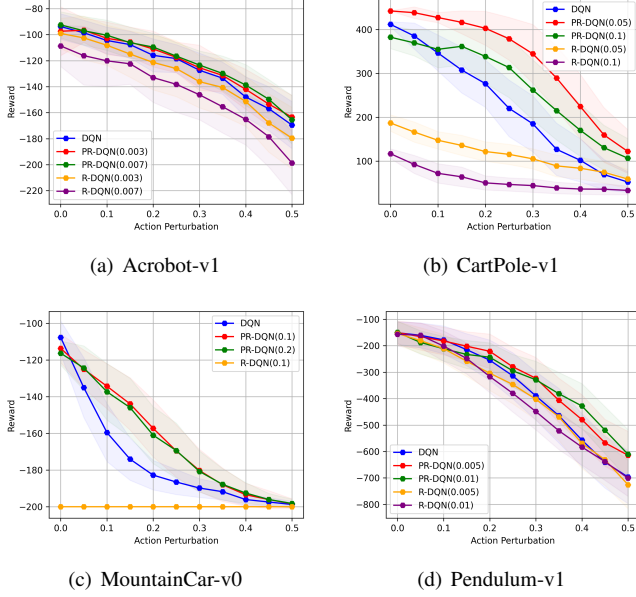


Fig. 4. Performance comparisons of various function-approximation methods under action perturbations.

This type of perturbation can occur in real-world applications. For example, when an agent’s observation is different to the environment’s state, action taken from the agent might not be optimal action. Moreover, it is also possible that in the application of autonomous driving, agent’s action can be performed with some noises. Second, in parameter perturbation, the parameter setting in training environment can be different from that in testing environment. This type of perturbation can well represent the mismatches between simulator model and real-world settings. To see the impact of robustness-level  $R$ , we choose two different values of  $R$  except the vanilla methods. An agent is trained with five instances for each method. At evaluation time step, we take the average reward and standard deviation of 100 times tests for each instance. In every figure, the thick line represents the average value and light region shows  $\pm 0.5$  standard deviation. We provide more details for simulation settings (e.g., hyperparameter setting) and additional experiment results under various parameter perturbations in the supplementary.

Figure 2 shows that the proposed PRQ-Learning provides the robustness against action perturbations, whereas the benchmark methods seem to be failed. We can identify the reason from Figure 3, where red-box denotes the cliff that gives the highest cost to the agent. We can see that the agent trained with Q-Learning takes actions so that it moves right above the cliff (i.e., the shortest path to reach the goal). However, the agents trained with ARQ and PRQ-Learning take actions so that it tends to choose the path far from the cliff. This indeed shows that ARQ and PRQ-Learning can learn some possible dangers of adjacent states. Also, it is verified that  $V_t^\pi(x_{t+1})$  in (12) indeed solves the maximization in (7) (see Figure 1 in Appendix D).

We can see that the agent trained with Robust-Q is failed to learn a robust action. This is because the agent is learned by

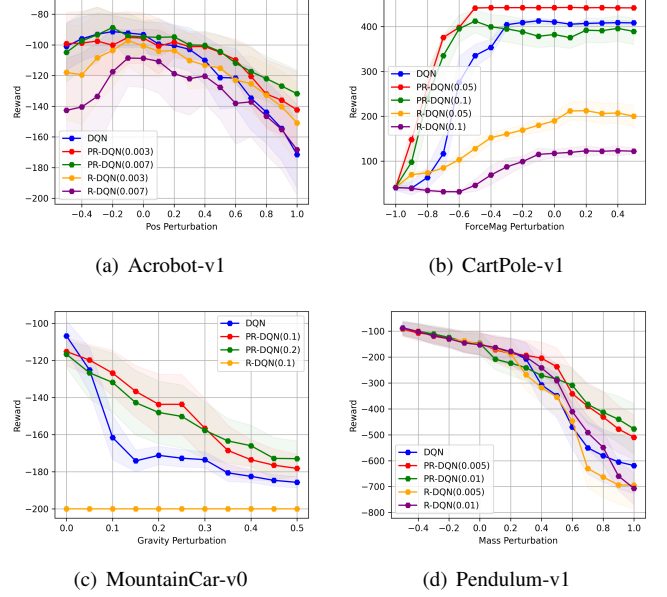


Fig. 5. Performance comparisons of various function-approximation methods under parameter perturbations.

considering the dangers of the entire states rather than those of neighboring states. Namely, this agent overestimates possible dangers in the environment.

From Figures 4 and 6, focusing on continuous state and/or action spaces, we conduct the experiments of function-approximation methods. The proposed PR-DQN and PR-DDPG achieve higher rewards than the benchmark methods such as DQN, R-DQN, DDPG, and R-DDPG in the presence of perturbations (i.e., training and testing environments are different). Remarkably, although the proposed methods are trained basically against action perturbations, they still show greater rewards in parameter perturbations. There are some cases that vanilla RL methods achieve higher rewards than the proposed methods in non-perturbation situations. But, it is reasonable because in this case, training and testing environments are identical. When perturbations are applied, the proposed methods attain higher rewards than the vanilla methods. Like tabular case, the proposed methods outperform the benchmark robust methods such as R-DQN and R-DDPG, by ensuring better robustness to the perturbations in environment. These results strengthen our argument that the proposed uncertainty set better reflects real-world perturbations (or uncertainties).

## VII. CONCLUSION

We presented the novel uncertainty set which better reflects real-world perturbations than the existing sets. Using this, we first design ARQ-Learning for tabular case and theoretically characterized its performance. Pessimistic agent was presented, which tackles the key bottleneck for the extension of ARQ-Learning into continuous state spaces. Using this technique, we constructed PRQ-Learning for tabular case, and PR-DQN and PR-DDPG for continuous state space. While the proposed methods are based on DQN and DDPG as the baseline RL methods, we remark that the key idea to use pes-

simistic agent can be easily integrated with the other model-free RL methods. Experiments demonstrated the superiority of the proposed methods.

#### APPENDIX A PROOF OF THEOREM 1

In this section we show the proof of Theorem 1. It was shown in [12] that robust Bellman operator is contraction. In addition, [9] shows contraction of robust Bellman operator for  $R$ -contamination set. Here, we extend this to *adjacent*  $R$ -contamination uncertainty set. In below analysis, we assume that neighboring set of state  $s$  at least include  $s$  as its element  $s \in \mathcal{N}_s$  to ensure that neighboring set isn't empty set  $\mathcal{N}_s \neq \emptyset$ . This is proper assumption because if an agent don't take any action, it can stay its previous state with non-zero probability.

$$\begin{aligned}
& |\mathbf{T}Q_1(s, a) - \mathbf{T}Q_2(s, a)| \\
&= \left| c(s, a) + \gamma(1 - R) \left[ \sum_{s' \in S} \bar{p}_{s, s'}^a V_1(s') \right] + \gamma R \left[ \max_{s' \in \mathcal{N}_s} V_1(s') \right] \right. \\
&\quad \left. - c(s, a) - \gamma(1 - R) \left[ \sum_{s' \in S} \bar{p}_{s, s'}^a V_2(s') \right] - \gamma R \left[ \max_{s' \in \mathcal{N}_s} V_2(s') \right] \right| \\
&= \left| \gamma(1 - R) \left[ \sum_{s' \in S} \bar{p}_{s, s'}^a (V_1(s') - V_2(s')) \right] \right. \\
&\quad \left. + \gamma R \left( \max_{s' \in \mathcal{N}_s} V_1(s') - \max_{s' \in \mathcal{N}_s} V_2(s') \right) \right| \\
&\leq \left| \gamma(1 - R) \left[ \sum_{s' \in S} \bar{p}_{s, s'}^a \left( \min_a Q_1(s', a) - \min_a Q_2(s', a) \right) \right] \right| \\
&\quad + \left| \gamma R \max_{s' \in \mathcal{N}_s} (V_1(s') - V_2(s')) \right| \\
&\leq \gamma(1 - R) \sum_{s' \in S} \bar{p}_{s, s'}^a \left| \min_a Q_1(s', a) - \min_a Q_2(s', a) \right| \\
&\quad + \gamma R \max_{s' \in \mathcal{N}_s} |V_1(s') - V_2(s')| \\
&\stackrel{(a)}{\leq} \gamma(1 - R) \|Q_1 - Q_2\|_\infty + \gamma R \|Q_1 - Q_2\|_\infty \\
&\leq \gamma \|Q_1 - Q_2\|_\infty
\end{aligned} \tag{17}$$

where (a) can be shown as

if  $\min_a Q_1(s', a) \geq \min_a Q_2(s', a)$ , then

$$\begin{aligned}
\left| \min_a Q_1(s', a) - \min_a Q_2(s', a) \right| &= \min_a Q_1(s', a) \\
&\quad - \min_a Q_2(s', a) \\
&\leq Q_1(s', b) - Q_2(s', b) \\
&\leq \|Q_1 - Q_2\|_\infty
\end{aligned} \tag{18}$$

where  $b = \operatorname{argmin}_a Q_2(s', a)$ .

And if  $\min_a Q_1(s', a) < \min_a Q_2(s', a)$ , then

$$\begin{aligned}
\left| \min_a Q_1(s', a) - \min_a Q_2(s', a) \right| &= \min_a Q_2(s', a) \\
&\quad - \min_a Q_1(s', a) \\
&\leq Q_2(s', c) - Q_1(s', c) \\
&\leq \|Q_1 - Q_2\|_\infty
\end{aligned} \tag{19}$$

where  $c = \operatorname{argmin}_a Q_1(s', a)$ . And,

$$\begin{aligned}
\max_{s' \in \mathcal{N}_s} |V_1(s') - V_2(s')| &\leq \max_{s' \in S} |V_1(s') - V_2(s')| \\
&\leq \|Q_1 - Q_2\|_\infty
\end{aligned} \tag{20}$$

So, we proved that our robust bellman operator  $\mathbf{T}$  is contraction with respect to  $l_\infty$ -norm. And using Banach fixed point theorem [32], we can see that  $Q^\pi$  is unique fixed point of  $\mathbf{T}$ .

#### APPENDIX B PROOF OF THEOREM 2

In this section we show proof of Theorem 2. As in Appendix A, we can assume that estimated neighboring set  $\hat{\mathcal{N}}_s$  is not empty set  $\hat{\mathcal{N}}_s \neq \emptyset$ . We first introduce vector notations.  $V_t \in \mathbb{R}^{|\mathcal{S}|}$ ,  $Q_t \in \mathbb{R}^{|\mathcal{S}| \times |\mathcal{A}|}$  represent vector representation of estimation of value functions at time steps  $t$ .  $V^* \in \mathbb{R}^{|\mathcal{S}|}$ ,  $Q^* \in \mathbb{R}^{|\mathcal{S}| \times |\mathcal{A}|}$  represent vector representation of optimal value function.  $c \in \mathbb{R}^{|\mathcal{S}| \times |\mathcal{A}|}$  denote vector representation of cost function so the  $(s, a)$  entry of  $c$  is cost received at  $(s, a)$ . We define transition kernel vector  $P_s^a \in \mathbb{R}^{|\mathcal{S}|}$  for given  $(s, a)$  as

$$P_s^a(s') = \bar{p}_{s, s'}^a \tag{21}$$

For given sample  $O_t = (s_t, a_t, s_{t+1})$ , we can define the sample transition vector  $P_{s, t+1}^a \in \mathbb{R}^{|\mathcal{S}|}$  as

$$P_{s, t+1}^a(s') = \begin{cases} 1, & \text{if } (s, a, s') = O_t \\ 0, & \text{o.w.} \end{cases} \tag{22}$$

Using above vector notation, we can express the update of  $ARQ$ -learning at  $(s, a)$ -th element as

$$\begin{aligned}
Q_t(s, a) &= (1 - \alpha \mathbb{1}_{s=s_t}) Q_{t-1}(s, a) \\
&\quad + \alpha \mathbb{1}_{s=s_t} \left( c(s, a) + \gamma(1 - R) (P_{s, t}^a)^\top V_{t-1} + \gamma R \max_{s' \in \hat{\mathcal{N}}_s} V_{t-1}(s') \right) \\
&= (1 - \alpha \mathbb{1}_{s=s_t}) Q_{t-1}(s, a) \\
&\quad + \alpha \mathbb{1}_{s=s_t} \left( c(s, a) + \gamma(1 - R) (P_{s, t}^a)^\top V_{t-1} + \gamma R \max_{s' \in \hat{\mathcal{N}}_s} V_{t-1}(s') \right)
\end{aligned} \tag{23}$$

where  $\mathbb{1}$  indicates indicator function. Equation (24) is same as (23) because of indicator function  $\mathbb{1}_{s=s_t}$ . The optimal robust bellman equation can be written as

$$Q^*(s, a) = c(s, a) + \gamma(1 - R) (P_s^a)^\top V^* + \gamma R \max_{s' \in \hat{\mathcal{N}}_s} V^*(s) \tag{25}$$



Define  $\psi_t(s, a) = Q_t(s, a) - Q^*(s, a)$ , then

$$\begin{aligned}
\psi_t(s, a) &= Q_t(s, a) - Q^*(s, a) \\
&= (1 - \alpha \mathbb{1}_{s=s_t}) (Q_{t-1}(s, a) - Q^*(s, a)) \\
&\quad + \alpha \mathbb{1}_{s=s_t} (Q_t(s, a) - Q^*(s, a)) \\
&= (1 - \alpha \mathbb{1}_{s=s_t}) \psi_{t-1}(s, a) \\
&\quad + \alpha \mathbb{1}_{s=s_t} \gamma (1 - R) ((P_{s,t}^a)^\top V_{t-1} - (P_s^a)^\top V^*) \\
&\quad + \alpha \mathbb{1}_{s=s_t} \gamma R \left( \max_{s \in \tilde{\mathcal{N}}_s} V_{t-1}(s) - \max_{s \in \tilde{\mathcal{N}}_s} V^*(s) \right) \\
&= (1 - \alpha \mathbb{1}_{s=s_t}) \psi_{t-1}(s, a) \\
&\quad + \alpha \gamma (1 - R) \mathbb{1}_{s=s_t} ((P_{s,t}^a)^\top V_{t-1} - (P_{s,t}^a)^\top V^*) \\
&\quad + \alpha \gamma (1 - R) \mathbb{1}_{s=s_t} ((P_{s,t}^a)^\top V^* - (P_s^a)^\top V^*) \\
&\quad + \alpha \gamma R \mathbb{1}_{s=s_t} \left( \max_{s \in \tilde{\mathcal{N}}_s} V_{t-1}(s) - \max_{s \in \tilde{\mathcal{N}}_s} V^*(s) \right) \\
&= (1 - \alpha \mathbb{1}_{s=s_t}) \psi_{t-1}(s, a) \\
&\quad + \alpha \gamma (1 - R) \mathbb{1}_{s=s_t} (P_{s,t}^a - P_s^a)^\top V^* \\
&\quad + \alpha \gamma (1 - R) \mathbb{1}_{s=s_t} (P_{s,t}^a)^\top (V_{t-1} - V^*) \\
&\quad + \alpha \gamma R \mathbb{1}_{s=s_t} \left( \max_{s \in \tilde{\mathcal{N}}_s} V_{t-1}(s) - \max_{s \in \tilde{\mathcal{N}}_s} V^*(s) \right)
\end{aligned} \tag{26}$$

Applying this relation recursively gives

$$\psi_t(s, a) = \beta_{1,t}(s, a) + \beta_{2,t}(s, a) + \beta_{3,t}(s, a) \tag{27}$$

where  $\beta_{1,t}(s, a)$ ,  $\beta_{2,t}(s, a)$ , and  $\beta_{3,t}(s, a)$  are defined as

$$\beta_{1,t}(s, a) = \prod_{j=1}^t (1 - \mathbb{1}_{s=s_j}) \psi_0(s, a) \tag{28}$$

$$\begin{aligned}
\beta_{2,t}(s, a) &= \gamma (1 - R) \sum_{i=1}^t \prod_{j=i+1}^t (1 - \mathbb{1}_{s=s_j}) \mathbb{1}_{s=s_i} \\
&\quad \cdot (P_{s,i}^a - P_s^a)^\top V^*
\end{aligned} \tag{29}$$

$$\begin{aligned}
\beta_{3,t}(s, a) &= \gamma (1 - R) \sum_{i=1}^t \prod_{j=i+1}^t (1 - \mathbb{1}_{s=s_j}) \mathbb{1}_{s=s_i} \\
&\quad \cdot (P_{s,i}^a)^\top (V_{i-1} - V^*) \\
&\quad + \gamma R \sum_{i=1}^t \prod_{j=i+1}^t (1 - \mathbb{1}_{s=s_j}) \mathbb{1}_{s=s_i} \\
&\quad \cdot \left( \max_{s \in \tilde{\mathcal{N}}_s} V_{i-1}(s) - \max_{s \in \tilde{\mathcal{N}}_s} V^*(s) \right)
\end{aligned} \tag{30}$$

Using triangle inequality, we can obtain bound of  $\psi_t(s, a)$  as

$$|\psi_t(s, a)| \leq |\beta_{1,t}(s, a)| + |\beta_{2,t}(s, a)| + |\beta_{3,t}(s, a)| \tag{31}$$

Now, we derive bound of each term  $\beta_{1,t}(s, a)$ ,  $\beta_{2,t}(s, a)$ , and  $\beta_{3,t}(s, a)$ .

**Lemma 1.**

For any  $\delta > 0$ , and  $t_{\text{frame}} = \frac{443t_{\text{mix}}}{\mu_{\min}} \log \left( \frac{4|\mathcal{S}||\mathcal{A}|T}{\delta} \right)$ . Suppose that  $t_{\text{frame}} \leq T$ . Then with probability at least  $1 - \delta$ ,  $\beta_{1,t}(s, a)$  is bounded as

$$|\beta_{1,t}(s, a)| \leq (1 - \alpha)^{\frac{1}{2}t\mu_{\min}} \|\psi_0\|_\infty \quad t_{\text{frame}} < \forall t < T \tag{32}$$

$$|\beta_{1,t}(s, a)| \leq \|\psi_0\|_\infty \quad \forall t < t_{\text{frame}} \tag{33}$$

for all  $(s, a) \in \mathcal{S} \times \mathcal{A}$

This bound is exactly same as bound given in Lemma 2 in [25] and bound given in Lemma 1 in [9]. So, proof of Lemma 1 can be obtained in [25] and [9].

**Lemma 2.**

There exists some constant  $c > 0$  such that for any  $0 < \delta < 1$  and  $t \leq T$  that satisfies  $0 < \alpha \log \frac{|\mathcal{S}||\mathcal{A}|T}{\delta} < 1$ , with probability at least  $1 - \delta$ ,

$$\begin{aligned}
|\beta_{2,t}(s, a)| &\leq c\gamma(1 - R) \sqrt{\eta \log \left( \frac{|\mathcal{S}||\mathcal{A}|T}{\delta} \right)} \|V^*\|_\infty \\
&\leq c\gamma \sqrt{\eta \log \left( \frac{|\mathcal{S}||\mathcal{A}|T}{\delta} \right)} \|V^*\|_\infty
\end{aligned} \tag{34}$$

is satisfied for all  $(s, a) \in \mathcal{S} \times \mathcal{A}$

This bound is exactly same as bound given in Lemma 1 in [25]. So, proof of Lemma 2 can be obtained in [25].

**Lemma 3.**

For any  $t > 0$ ,

$$|\beta_{3,t}(s, a)| \leq \gamma \sum_{i=1}^t \|\psi_{t-1}\|_\infty \prod_{j=i+1}^t (1 - \mathbb{1}_{s=s_j}) \mathbb{1}_{s=s_i} \tag{35}$$

is satisfied for all  $(s, a) \in \mathcal{S} \times \mathcal{A}$

**Proof**

$$\begin{aligned}
|(P_{s,i}^a)^\top (V_{i-1} - V^*)| &\leq \|P_{s,i}^a\|_\infty \|V_{i-1} - V^*\|_\infty \\
&\leq \|V_{i-1} - V^*\|_\infty \\
&= \max_s |V_{i-1}(s) - V^*(s)| \\
&= |V_{i-1}(s^*) - V^*(s^*)| \\
&= \left| \min_a Q_{i-1}(s^*, a) - \min_b Q^*(s^*, b) \right| \\
&\leq \|Q_{i-1} - Q^*\|_\infty \\
&= \|\psi_{i-1}\|_\infty
\end{aligned} \tag{36}$$

where  $s^* = \arg \max |V_{i-1}(s) - V^*(s)|$

$$\begin{aligned}
\left| \max_{s \in \tilde{\mathcal{N}}_s} V_{i-1}(s) - \max_{s \in \tilde{\mathcal{N}}_s} V^*(s) \right| &\leq \|V_{i-1} - V^*\|_\infty \\
&\leq \|Q_{i-1} - Q^*\|_\infty \\
&= \|\psi_{i-1}\|_\infty
\end{aligned} \tag{37}$$

It is natural that  $0 \leq (1 - \mathbb{1}_{s=s'}) \leq 1$  and  $0 \leq \mathbb{1}_{s=s'} \leq 1$  for all  $s, s' \in \mathcal{S}$ . So,

$$|\beta_{3,t}(s, a)| \leq \gamma \sum_{i=1}^t \|\psi_{t-1}\|_\infty \prod_{j=i+1}^t (1 - \mathbb{1}_{s=s_j}) \mathbb{1}_{s=s_i} \tag{38}$$

Now we combine the bounds for terms  $\beta_{1,t}(s, a)$ ,  $\beta_{2,t}(s, a)$ ,  $\beta_{3,t}(s, a)$ . Then we can get bound of  $\psi_t(s, a)$  as

For  $t < t_{\text{frame}}$

$$\begin{aligned}
|\psi_t(s, a)| &\leq \|\psi_0\|_\infty + \gamma c \sqrt{\alpha \log \frac{|\mathcal{S}||\mathcal{A}|T}{\delta}} \|V^*\|_\infty \\
&\quad + \gamma \sum_{i=1}^t \|\psi_{i-1}\|_\infty \prod_{j=i+1}^t (1 - \mathbb{1}_{s=s_j}) \mathbb{1}_{s=s_i}
\end{aligned} \tag{39}$$

and for  $t_{\text{frame}} \leq t \leq T$

$$|\psi_t(s, a)| \leq (1 - \alpha)^{\frac{t\mu_{\min}}{2}} \|\psi_0\|_{\infty} + \gamma c \sqrt{\alpha \log \frac{|S||A|T}{\delta}} \|V^*\|_{\infty} + \gamma \sum_{i=1}^t \|\psi_{i-1}\|_{\infty} \prod_{j=i+1}^t (1 - \mathbb{I}_{s=s_j}) \mathbb{I}_{s=s_i} \quad (40)$$

This bound exactly matches the bound in Equation (47) in [25] and bound in Equation (51), (52) in [9], so remaining proof for Theorem 2 can be obtained by following proof in [25], [9].

## APPENDIX C ALGORITHMS

In this section, we provide the detailed procedures of the proposed PR-DQN and PR-DDPG in Algorithm 1 and Algorithm 2, respectively.

### Algorithm 3 PR-DQN

```

1: Input: Learning rate  $\lambda_Q > 0$ , discounted factor  $\gamma \in (0, 1)$ ,
   robustness-level  $R$ , and  $\tau > 0$ .
2: Initialization:  $\psi, \bar{\psi}, \omega, \bar{\omega}, s_0 \in \mathcal{S}$ .
3: for each epoch do
4:   for each environment step do
5:      $x_t \leftarrow s_t$ 
6:      $a_t \sim \pi(s_t), u_t \sim \phi(x_t), s_{t+1} \sim \bar{p}_{s_t}^{a_t}$  and  $x_{t+1} \sim \bar{p}_{x_t}^{u_t}$ 
7:      $\mathcal{D} \leftarrow \mathcal{D} \cup \{(s_t, a_t, c_t = c(s_t, a_t), s_{t+1}, u_t, c_t^p = -c(x_t, u_t), x_{t+1})\}$ 
8:      $s_t \leftarrow s_{t+1}$ 
9:   end for
10:  for each update step do
11:     $(s, a, c, s', u, c^p, x') \sim \mathcal{D}$ 
12:     $\bar{V}^{\pi}(x') = \min_{a' \in \mathcal{A}} \bar{Q}^{\pi}(x', a')$ 
13:     $\bar{V}^{\pi}(s') = \min_{a' \in \mathcal{A}} \bar{Q}^{\pi}(s', a')$ 
14:     $\bar{V}^{\phi}(x') = \min_{u' \in \mathcal{A}} \bar{Q}^{\phi}(x', u')$ 
15:     $\psi \leftarrow \psi - \lambda_Q \nabla_{\psi} J_{Q^{\phi}}(\psi)$ 
16:     $\omega \leftarrow \omega - \lambda_Q \nabla_{\omega} J_{Q^{\pi}}(\omega)$ 
17:     $\bar{\psi} \leftarrow \tau \psi + (1 - \tau) \bar{\psi}$ 
18:     $\bar{\omega} \leftarrow \tau \omega + (1 - \tau) \bar{\omega}$ 
19:  end for
20: end for

```

## APPENDIX D EXPERIMENTS

In this section, we provide details for simulation settings and additional experiments.

### A. Policy

We are using  $\epsilon$ -greedy policy for tabular methods, discrete action space algorithms.  $\epsilon$ -policy is defined as

$$\pi(s) = \begin{cases} \text{random action} & \text{with probability } \epsilon \\ \arg\max_a Q(s, a) & \text{with probability } 1 - \epsilon \end{cases} \quad (41)$$

### Algorithm 4 PR-DDPG

```

1: Input: Learning rate  $\lambda_Q > 0, \lambda_p > 0$ , discounted factor
    $\gamma \in (0, 1)$ , robustness-level  $R$ , and  $\tau > 0$ .
2: Initialization:  $\theta, \bar{\theta}, \sigma, \bar{\sigma}, \psi, \bar{\psi}, \omega, \bar{\omega}, s_0 \in \mathcal{S}$ .
3: for each epoch do
4:   for each environment step do
5:      $x_t \leftarrow s_t$ 
6:      $a_t \sim \pi(s_t), u_t \sim \phi(x_t), s_{t+1} \sim \bar{p}_{s_t}^{a_t}$  and  $x_{t+1} \sim \bar{p}_{x_t}^{u_t}$ 
7:      $\mathcal{D} \leftarrow \mathcal{D} \cup \{(s_t, a_t, c_t = c(s_t, a_t), s_{t+1}, u_t, c_t^p = -c(x_t, u_t), x_{t+1})\}$ 
8:      $s_t \leftarrow s_{t+1}$ 
9:   end for
10:  for each update step do
11:     $(s, a, c, s', u, c^p, x') \sim \mathcal{D}$ 
12:     $a'_1 \sim \bar{\pi}(s'), a'_2 \sim \bar{\pi}(x')$  and  $u' \sim \bar{\phi}(x')$ 
13:     $\bar{V}^{\pi}(x') = \bar{Q}^{\pi}(x', a'_2)$ 
14:     $\bar{V}^{\pi}(s') = \bar{Q}^{\pi}(s', a'_1)$ 
15:     $\bar{V}^{\phi}(x') = \bar{Q}^{\phi}(x', u')$ 
16:     $\psi \leftarrow \psi - \lambda_Q \nabla_{\psi} J_{Q^{\phi}}(\psi)$ 
17:     $\omega \leftarrow \omega - \lambda_Q \nabla_{\omega} J_{Q^{\pi}}(\omega)$ 
18:     $\sigma \leftarrow \sigma - \lambda_p \nabla_{\sigma} J_{\pi}(\sigma)$ 
19:     $\theta \leftarrow \theta - \lambda_p \nabla_{\theta} J_{\pi}(\theta)$ 
20:     $\bar{\psi} \leftarrow \tau \psi + (1 - \tau) \bar{\psi}$ 
21:     $\bar{\omega} \leftarrow \tau \omega + (1 - \tau) \bar{\omega}$ 
22:     $\bar{\theta} \leftarrow \tau \theta + (1 - \tau) \bar{\theta}$ 
23:     $\bar{\sigma} \leftarrow \tau \sigma + (1 - \tau) \bar{\sigma}$ 
24:  end for
25: end for

```

	FrozenLake-v1	CliffWalking-v0
$\gamma$	0.99	0.99
$\alpha$	0.01	0.01
Batch Size	32	32
Buffer Size	20000	20000
Max Episode times	4000	1000

TABLE I  
HYPER PARAMETERS FOR TABULAR ALGORITHMS

	Acrobot-v1	CartPole-v1
Hidden Layers	[64, 64]	[64, 64]
$\gamma$	0.99	0.99
$\tau$	0.01	0.01
Batch Size	32	32
Buffer Size	20000	20000
Learning Rate	0.0001	0.001
Max Episode times	500	1000
Train Reward Function	.	.
Value Memory Size	32*30	32*30

TABLE II  
HYPER PARAMETERS FOR FUNCTION APPROXIMATION ALGORITHMS

### B. Hyperparameter settings

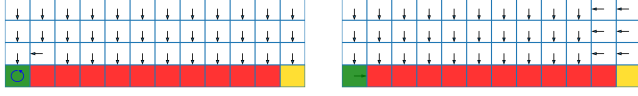
Here, A means actor, C means critic, and  $f(s)$  is defined as

$$f(s) = \begin{cases} 2, & \text{if } 0.5 \leq s(0) \\ (s(0) + 1.2)/1.8 - 1, & \text{o.w.} \end{cases} \quad (42)$$

	MountainCar-v0	Pendulum-v1
<b>Hidden Layers</b>	[64, 64]	[256, 256]
$\gamma$	0.99	0.99
$\tau$	0.01	0.05
<b>Batch Size</b>	32	32
<b>Buffer Size</b>	20000	20000
<b>Learning Rate</b>	0.001	0.0001(A), 0.001(C)
<b>Max Episode times</b>	2000	300
<b>Train Reward Function</b>	$f(s)$	.
<b>Value Memory Size</b>	32*30	32*30

TABLE III

HYPER PARAMETERS FOR FUNCTION APPROXIMATION ALGORITHMS



(a) Max state among elements in  $\hat{N}_s$  in ARQ-Learning (b) Max state obtained by pessimistic agent in PRQ-Learning

Fig. 6. We represent estimated maximum state  $s^* = \arg\max_{s' \in \hat{N}_s} V^\pi(s')$  in (a) and  $x' \sim \tilde{p}_x^{u^*}$  in (b) for all  $s, x \in \mathcal{S}$  in CliffWalking-v0 ( $u^*$  represents optimal action of pessimistic agent). Arrow points out maximum state in neighboring set estimated by each methods.

We use different reward function for MountainCar-v0 during training to increase learning speed. With original reward function, an agent doesn't get any reward signal from environment until it reaches to goal position. So, reaching to goal position totally depends on random action. And, it takes too long time in most cases. By using given reward function, however, we can accelerate learning speed.

### C. Additional Experiments

In this section, we provide various simulation results to verify superiority of our proposed methods.

First, we show that pessimistic agent of PRQ-Learning actually can solve maximization in robust Bellman operator in equation (7) in main text.

As you see in Fig 6, maximum state found by pessimistic agent of PRQ-Learning almost same as maximum state found in  $\hat{N}_s$  in ARQ-Learning. So, we can sure that pessimistic agent can really solve maximization in equation (7) in main text. Also, we can see that arrows in both of figures are pointing in the direction of cliff. This means that both of way can detect some danger in environment. By applying this danger to update equation in Q-network, we can give robustness to the agent.

Next, we provide result of FrozenLake environment with slippery.

For the case of FrozenLake with slippery, an agent take random action with probability 0.66 and take designed action with probability 0.33. This means that this environment has inherently uncertain characteristic. So, even without specific robust RL algorithm, an agent can learn robust action. We can see every algorithms show almost similar reward according to action perturbations in Figure 7.

Finally, we provide results of function approximation algorithms according to various parameter perturbations. From

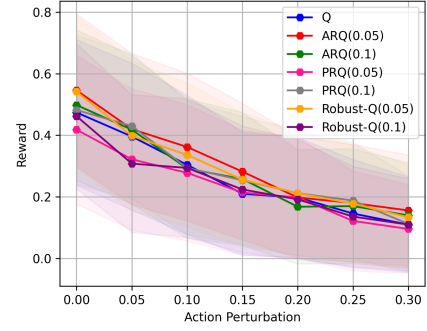
Fig. 7. FrozenLake-v1( $8 \times 8$ ) with slippery

Fig. 8 to 10, we can see PR-DQN, PR-DDPG surpass DQN, DDPG in most of parameter perturbation simulations. Our methods even show great reward compared to R-DQN, R-DDPG which use  $R$ -contamination uncertainty set. So, we can sure our proposed *adjacent*  $R$ -contamination uncertainty set is more elaborate than previous ones.

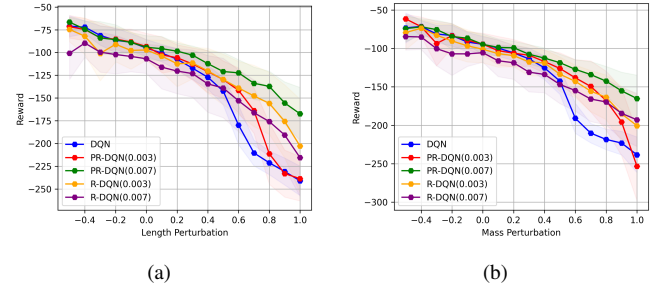


Fig. 8. Result of function approximation algorithms in Acrobot-v1 under parameter perturbations.

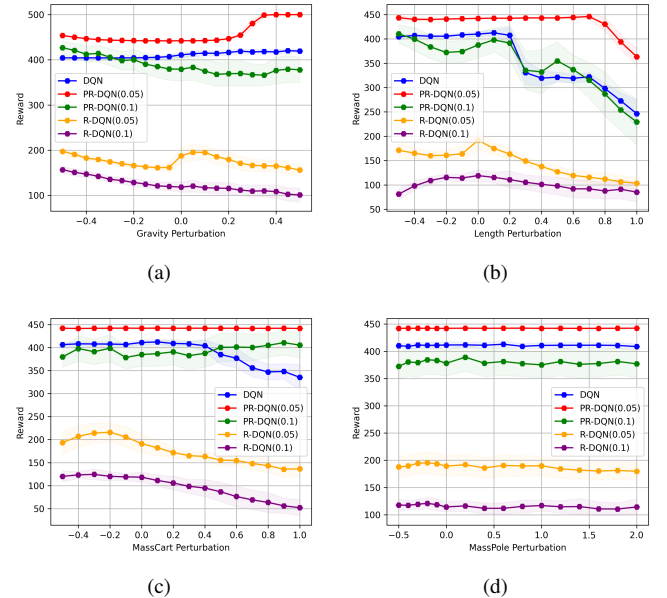


Fig. 9. Result of function approximation algorithms in CartPole-v1 under parameter perturbations.

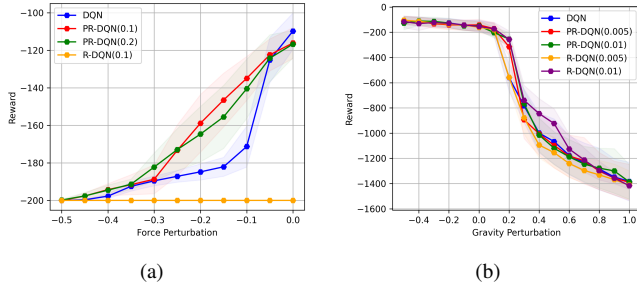


Fig. 10. Result of function approximation algorithms in MountainCar-v0 and Pendulum-v1 under parameter perturbations.

## REFERENCES

- [1] R. S. Sutton and A. G. Barto, *Reinforcement learning: An introduction*. MIT press, 2018.
- [2] C. Szepesvári, “Algorithms for reinforcement learning,” *Synthesis lectures on artificial intelligence and machine learning*, vol. 4, no. 1, pp. 1–103, 2010.
- [3] L. Pinto, J. Davidson, R. Sukthankar, and A. Gupta, “Robust adversarial reinforcement learning,” in *International Conference on Machine Learning*, pp. 2817–2826, PMLR, 2017.
- [4] A. Gleave, M. Dennis, C. Wild, N. Kant, S. Levine, and S. Russell, “Adversarial policies: Attacking deep reinforcement learning,” *arXiv preprint arXiv:1905.10615*, 2019.
- [5] S. Li, Y. Wu, X. Cui, H. Dong, F. Fang, and S. Russell, “Robust multi-agent reinforcement learning via minimax deep deterministic policy gradient,” in *Proceedings of the AAAI conference on artificial intelligence*, vol. 33, pp. 4213–4220, 2019.
- [6] H. Zhang, H. Chen, D. Boning, and C.-J. Hsieh, “Robust reinforcement learning on state observations with learned optimal adversary,” *arXiv preprint arXiv:2101.08452*, 2021.
- [7] A. Roy, H. Xu, and S. Pokutta, “Reinforcement learning under model mismatch,” *Advances in neural information processing systems*, vol. 30, 2017.
- [8] K. P. Badrinath and D. Kalathil, “Robust reinforcement learning using least squares policy iteration with provable performance guarantees,” in *International Conference on Machine Learning*, pp. 511–520, PMLR, 2021.
- [9] Y. Wang and S. Zou, “Online robust reinforcement learning with model uncertainty,” *Advances in Neural Information Processing Systems*, vol. 34, pp. 7193–7206, 2021.
- [10] Y. Wang and S. Zou, “Policy gradient method for robust reinforcement learning,” in *International Conference on Machine Learning*, pp. 23484–23526, PMLR, 2022.
- [11] A. Nilim and L. El Ghaoui, “Robust control of markov decision processes with uncertain transition matrices,” *Operations Research*, vol. 53, no. 5, pp. 780–798, 2005.
- [12] G. N. Iyengar, “Robust dynamic programming,” *Mathematics of Operations Research*, vol. 30, no. 2, pp. 257–280, 2005.
- [13] E. Delage and S. Mannor, “Percentile optimization for markov decision processes with parameter uncertainty,” *Operations research*, vol. 58, no. 1, pp. 203–213, 2010.
- [14] W. Wiesemann, D. Kuhn, and B. Rustem, “Robust markov decision processes,” *Mathematics of Operations Research*, vol. 38, no. 1, pp. 153–183, 2013.
- [15] H. Xu and S. Mannor, “Distributionally robust markov decision processes,” *Advances in Neural Information Processing Systems*, vol. 23, 2010.
- [16] D. L. Kaufman and A. J. Schaefer, “Robust modified policy iteration,” *INFORMS Journal on Computing*, vol. 25, no. 3, pp. 396–410, 2013.
- [17] A. Tamar, S. Mannor, and H. Xu, “Scaling up robust mdps using function approximation,” in *International conference on machine learning*, pp. 181–189, PMLR, 2014.
- [18] P. J. Huber, “A robust version of the probability ratio test,” *The Annals of Mathematical Statistics*, pp. 1753–1758, 1965.
- [19] S. S. Du, Y. Wang, S. Balakrishnan, P. Ravikumar, and A. Singh, “Robust nonparametric regression under huber’s  $\epsilon$ -contamination model,” *arXiv preprint arXiv:1805.10406*, 2018.
- [20] E. M. Ronchetti and P. J. Huber, *Robust statistics*. John Wiley & Sons, 2009.
- [21] K. G. Nishimura and H. Ozaki, “Search and knightian uncertainty,” *Journal of Economic Theory*, vol. 119, no. 2, pp. 299–333, 2004.
- [22] K. G. Nishimura and H. Ozaki, “An axiomatic approach to  $\epsilon$ -contamination,” *Economic Theory*, vol. 27, no. 2, pp. 333–340, 2006.
- [23] A. Prasad, V. Srinivasan, S. Balakrishnan, and P. Ravikumar, “On learning using models under huber’s contamination model,” *Advances in neural information processing systems*, vol. 33, pp. 16327–16338, 2020.
- [24] A. Prasad, A. S. Suggala, S. Balakrishnan, and P. Ravikumar, “Robust estimation via robust gradient estimation,” *Journal of the Royal Statistical Society: Series B (Statistical Methodology)*, vol. 82, no. 3, pp. 601–627, 2020.
- [25] G. Li, Y. Wei, Y. Chi, Y. Gu, and Y. Chen, “Sample complexity of asynchronous q-learning: Sharper analysis and variance reduction,” *Advances in neural information processing systems*, vol. 33, pp. 7031–7043, 2020.
- [26] V. Mnih, K. Kavukcuoglu, D. Silver, A. A. Rusu, J. Veness, M. G. Bellemare, A. Graves, M. Riedmiller, A. K. Fidjeland, G. Ostrovski, et al., “Human-level control through deep reinforcement learning,” *nature*, vol. 518, no. 7540, pp. 529–533, 2015.
- [27] T. P. Lillicrap, J. J. Hunt, A. Pritzel, N. Heess, T. Erez, Y. Tassa, D. Silver, and D. Wierstra, “Continuous control with deep reinforcement learning,” *arXiv preprint arXiv:1509.02971*, 2015.
- [28] A. Nilim and L. Ghaoui, “Robustness in markov decision problems with uncertain transition matrices,” *Advances in neural information processing systems*, vol. 16, 2003.
- [29] T. Haarnoja, A. Zhou, P. Abbeel, and S. Levine, “Soft actor-critic: Off-policy maximum entropy deep reinforcement learning with a stochastic actor,” in *International conference on machine learning*, pp. 1861–1870, PMLR, 2018.
- [30] J. Schulman, F. Wolski, P. Dhariwal, A. Radford, and O. Klimov, “Proximal policy optimization algorithms,” *arXiv preprint arXiv:1707.06347*, 2017.
- [31] G. Brockman, V. Cheung, L. Pettersson, J. Schneider, J. Schulman, J. Tang, and W. Zaremba, “Openai gym,” *arXiv preprint arXiv:1606.01540*, 2016.
- [32] M. L. Puterman, *Markov decision processes: discrete stochastic dynamic programming*. John Wiley & Sons, 2014.